13th International Symposium on Turbulence and Shear Flow Phenomena (TSFP13)
Montreal, Canada, June 25–28, 2024

NEW LINEAR 3D OBLIQUE MODES - A NOVEL PATH TO TURBULENCE

M. Oberlack[1,2], **A. Yalcin**[1], **J. Laux**[1,2], **S. Görtz**[1,2], **L. De Broeck**[1,2], **Y. Wang**[1], **K. Wilhelm**[1,2]
[1]Chair of Fluid Dynamics, Technical University of Darmstadt, 64287 Darmstadt, Germany
[2]Center for Computational Engineering, Technical University of Darmstadt, 64293 Darmstadt, Germany
oberlack@fdy.tu-darmstadt.de

ABSTRACT

The Squire transformation, which is based on the temporal stability framework and which proves that the critical Reynolds number of 2D modes is always smaller than that of 3D modes, is extended to the spatial stability framework. Based on this extension, spatially developing 3D oblique modes can be formulated. A key result is that, in contrast to the classical Squire theorem, critical Reynolds numbers of 3D modes exist that may be lower than those for 2D modes. An instability condition is formulated in terms of the group velocity of each mode, that requires that the perturbation energy must always be transported in the direction of the increasing mode to represent an instability. The instability condition for 3D is formulated based solely on the corresponding 2D quantities. The spatial linear stability eigenvalue problem of plane Couette flow is investigated, and we show that both spatially unstable 2D and 3D modes exist for it.

INTRODUCTION

Plane Couette flow is assumed to be linearly stable at all Reynolds numbers. It was proven by Romanov (1973) that there are no (temporally) growing perturbations for any Reynolds number. In contrast, transition and turbulence is observed in experiments, for example by Tillmark & Alfredsson (1992), Daviaud *et al.* (1992), and Tillmark & Alfredsson (1993).

In his famous theorem, Squire (1933) elegantly proved that for parallel shear flows, 2D perturbations are more unstable than 3D perturbations in the case of (temporal) perturbations, i.e. they become unstable at smaller Reynolds number. This allows to consider only the 2D (temporal) perturbations in the stability analysis.

Interestingly enough, in the transition from laminar to turbulent flow, three-dimensional oblique structures have been observed in multiple canonical flows such as plane Couette flow, Taylor-Couette flow or plane Poiseuille flow (Prigent *et al.*, 2003; Tuckerman & Barkley, 2011; Tuckerman *et al.*, 2020).

The theory of spatially evolving 3D oblique modes proposed here tries to reconcile the apparent gap between the experimental instability and the theoretical (temporal) linear stability of plane Couette flow, as well as to describe oblique structures appearing in the transition from laminar to turbulent plane Couette flow, by extending the temporal stability theory to the spatial stability framework.

GOVERNING EQUATIONS

Let the motion of an incompressible Newtonian fluid be governed by the set of dimensionless Navier-Stokes equations

$$\boldsymbol{\nabla} \cdot \boldsymbol{u} = 0, \tag{1a}$$

$$\frac{\partial \boldsymbol{u}}{\partial t} + (\boldsymbol{u} \cdot \boldsymbol{\nabla})\boldsymbol{u} = -\boldsymbol{\nabla} p + \frac{1}{Re}\Delta \boldsymbol{u} \quad \text{with} \quad Re := \frac{\varrho U_0 L}{\mu}, \tag{1b}$$

where $\boldsymbol{u}$, p and Re denote the velocity field, the pressure field and the Reynolds number, which consists of the fluid density ϱ, the dynamic viscosity μ, a characteristic velocity U_0 and a characteristic length scale L.

In linear stability theory, the velocity field and the pressure field are assumed to be composed of laminar base fields $\boldsymbol{U}$ and P, which are superimposed with perturbation fields $\boldsymbol{u'}$ and p' with infinitesimal magnitude of order ϵ and higher-order terms

$$\boldsymbol{u} = \boldsymbol{U} + \epsilon \boldsymbol{u}' + \mathcal{O}(\epsilon^2), \tag{2a}$$

$$p = P + \epsilon p' + \mathcal{O}(\epsilon^2). \tag{2b}$$

Inserting this assumption into the Navier-Stokes equations (1) leads to the following set of equations sorted by order of ϵ

$$\mathcal{O}(\epsilon^0): \qquad \boldsymbol{\nabla} \cdot \boldsymbol{U} = 0, \tag{3a}$$

$$\frac{\partial \boldsymbol{U}}{\partial t} + (\boldsymbol{U} \cdot \boldsymbol{\nabla})\boldsymbol{U} = -\boldsymbol{\nabla} P + \frac{1}{Re}\Delta \boldsymbol{U}, \tag{3b}$$

$$\mathcal{O}(\epsilon^1): \qquad \boldsymbol{\nabla} \cdot \boldsymbol{u}' = 0, \tag{3c}$$

$$\frac{\partial \boldsymbol{u}'}{\partial t} + (\boldsymbol{U} \cdot \boldsymbol{\nabla})\boldsymbol{u}' + (\boldsymbol{u}' \cdot \boldsymbol{\nabla})\boldsymbol{U} = -\boldsymbol{\nabla} p' + \frac{1}{Re}\Delta \boldsymbol{u}', \tag{3d}$$

where terms of second and higher order are neglected.

Let a Cartesian coordinate system with coordinates (x, y, z) be introduced with $\boldsymbol{U} = (U, V, W)$ as the laminar base flow components and $\boldsymbol{u}' = (u', v', w')$ as the velocity perturbations. In parallel shear flows, the base flow consists of one velocity component depending only on the wall-normal coordinate y, i.e. $\boldsymbol{U} = (U(y), 0, 0)$. Inserting this into the set of governing equations (3c) and (3d), a single fourth-order differential equations in terms of the velocity perturbation in

y-direction, v' can be generated

$$\left[\left(\frac{\partial}{\partial t}+U\frac{\partial}{\partial x}\right)\Delta-\frac{\mathrm{d}^2U}{\mathrm{d}y^2}\frac{\partial}{\partial x}-\frac{1}{Re}\Delta^2\right]v'=0. \quad (4)$$

Let this function v' be reformulated by a normal mode approach consisting of a y-dependent amplitude function $\tilde{v}$ and an exponential of angular wave numbers α, β in x-, z-direction and an angular wave frequency ω in time t

$$v'(x,y,z,t)=\tilde{v}(y)e^{i(\alpha x+\beta z-\omega t)}. \quad (5)$$

This transforms the spatio-temporal PDE (4) into a frequency-domain ODE, called the Orr-Sommerfeld equation

$$\left[(i\alpha U-i\omega)\left(\frac{\mathrm{d}^2}{\mathrm{d}y^2}-(\alpha^2+\beta^2)\right)-i\alpha\frac{\mathrm{d}^2U}{\mathrm{d}y^2} -\frac{1}{Re}\left(\frac{\mathrm{d}^2}{\mathrm{d}y^2}-(\alpha^2+\beta^2)\right)^2\right]\tilde{v}=0. \quad (6)$$

(TEMPORAL) SQUIRE TRANSFORMATION

The classical Squire transformation assumes a temporal stability framework with a complex wave frequency $\omega \in \mathbb{C}$, $\omega=\omega_r+i\omega_i$ and real wave numbers $\alpha, \beta \in \mathbb{R}$. This means that the spatial distribution is assumed to be wave-like, with the frequency ω_r in time and wave numbers α, β in the x- and z-directions, and the perturbation modes grow with positive ω_i or decay with negative ω_i in time.

Let the Orr-Sommerfeld equation be formulated in 2D and 3D by introducing respective indices indicating the dimensions for the physical quantities, i.e. for 2D

$$\left[(i\alpha_{2D}U-i\omega_{2D})\left(\frac{\mathrm{d}^2}{\mathrm{d}y^2}-\alpha_{2D}^2\right)-i\alpha_{2D}\frac{\mathrm{d}^2U}{\mathrm{d}y^2} -\frac{1}{Re_{2D}}\left(\frac{\mathrm{d}^2}{\mathrm{d}y^2}-\alpha_{2D}^2\right)^2\right]\tilde{v}=0, \quad (7)$$

and for 3D

$$\left[(i\alpha_{3D}U-i\omega_{3D})\left(\frac{\mathrm{d}^2}{\mathrm{d}y^2}-(\alpha_{3D}^2+\beta^2)\right)-i\alpha_{3D}\frac{\mathrm{d}^2U}{\mathrm{d}y^2} -\frac{1}{Re_{3D}}\left(\frac{\mathrm{d}^2}{\mathrm{d}y^2}-(\alpha_{3D}^2+\beta^2)\right)^2\right]\tilde{v}=0. \quad (8)$$

It can be observed that both equations have the same parameter and hence the same solution space for the following set of invariance transformations, i.e.

$$\omega_{2D}Re_{2D}=\omega_{3D}Re_{3D}, \quad (9a)$$
$$\alpha_{2D}Re_{2D}=\alpha_{3D}Re_{3D}, \quad (9b)$$
$$\alpha_{2D}^2=\alpha_{3D}^2+\beta^2. \quad (9c)$$

By introducing a scaling parameter ϕ between the 2D and 3D Reynolds numbers, the 3D quantities can be expressed by the 2D quantities and vice versa

$$\phi := \frac{Re_{3D}}{Re_{2D}}, \quad (10a)$$
$$\omega_{3D}=\frac{\omega_{2D}}{\phi}, \quad (10b)$$
$$\alpha_{3D}=\frac{\alpha_{2D}}{\phi}, \quad (10c)$$
$$\beta=\pm\sqrt{1-\frac{1}{\phi^2}}\,\alpha_{2D}. \quad (10d)$$

Since $\alpha, \beta \in \mathbb{R}$ was assumed, it follows for the scaling parameter that $\phi > 1$. This means that for a 2D and a 3D flow in the same solution space, the 3D flow has a higher Reynolds number, or in other words: if there is a critical Reynolds number $Re_{2D,cr}$ in the 2D modes, it will always be lower than the corresponding critical 3D Reynolds number $Re_{3D,cr}$. This leads back to Squire's classical finding that the 2D modes are temporally more unstable, or in other words become unstable at smaller Reynolds numbers.

EXTENSION OF THE SQUIRE TRANSFORMATION TO SPATIAL FRAMEWORK

To extend the Squire transformation, a spatial stability framework is assumed with a real wave frequency $\omega \in \mathbb{R}$ and complex wave numbers $\alpha, \beta \in \mathbb{C}$, $\alpha=\alpha_r+i\alpha_i$ and $\beta=\beta_r+i\beta_i$. For this case, the real wave parameters α_r, β_r and ω describe the harmonics in space and time, while α_i and β_i stand for the growth or decay of the perturbation mode in the x- and z-direction. A positive imaginary part of the wave numbers corresponds here to spatial growth in negative x- and z-direction, while a negative imaginary part respectively means spatial growth in positive x- and z-direction.

Comparing once again the Orr-Sommerfeld equation in 2D and 3D, both have again the same solution space for the same set of invariance transformations as in the temporal framework (9), but this time, the third condition (9c) can be split into a real and an imaginary part, yielding overall

$$\omega_{2D}Re_{2D}=\omega_{3D}Re_{3D}, \quad (11a)$$
$$\alpha_{2D}Re_{2D}=\alpha_{3D}Re_{3D}, \quad (11b)$$
$$\alpha_{2D,r}^2-\alpha_{2D,i}^2=\alpha_{3D,r}^2-\alpha_{3D,i}^2+\beta_r^2-\beta_i^2, \quad (11c)$$
$$\alpha_{2D,r}\alpha_{2D,i}=\alpha_{3D,r}\alpha_{3D,i}+\beta_r\beta_i. \quad (11d)$$

By introducing the same scaling parameter ϕ as in the temporal stability framework, the 3D quantities can now be expressed again in terms of the 2D quantities and vice versa,

$$\omega_{3D}=\frac{\omega_{2D}}{\phi}, \quad (12a)$$
$$\alpha_{3D}=\frac{\alpha_{2D}}{\phi}, \quad (12b)$$

$$\beta=\begin{cases}\pm\sqrt{1-\frac{1}{\phi^2}}\,\alpha_{2D} & \text{for} \quad \phi>1, \quad (12c)\\ \mp i\sqrt{\frac{1}{\phi^2}-1}\,\alpha_{2D} & \text{for} \quad \phi<1. \quad (12d)\end{cases}$$

Now, there are two possible solution branches for β, depending on whether $\phi > 1$ or $\phi < 1$. The physically interesting case is $\phi < 1$, as this indicates the case, that a 2D flow has a higher Reynolds number than a 3D flow in the same solution space, or in other words: if there is a critical Reynolds number, it can appear first in 3D, as the 3D modes may be spatially more unstable. Only this case is investigated further on.

It is interesting to note that in this case, in the formulation for β for $\phi < 1$, the real and imaginary parts of α_{2D} swap roles, i.e. $\beta_r = \pm\sqrt{1/\phi^2 - 1}\,\alpha_{2D,i}$ and $\beta_i = \mp\sqrt{1/\phi^2 - 1}\,\alpha_{2D,r}$.

Since it is easier to compute eigenvalues or construct the analytical solution in 2D, the further investigated 3D modes are expressed by their corresponding 2D modes.

In contrast to temporal instabilities, the spatial growth rates α_i and β_i alone are not sufficient to decide on instability in the case of spatial instabilities. For spatial instabilities, the group velocity is an important property, i.e. the velocity at which energy is conveyed along a wave. There have been two competing definitions of this group velocity c_g, applicable to two distinct physical problems (Criminale *et al.*, 2010). Whereas $\partial\omega/\partial\alpha_r$ is widely used in the context of Gaster's transformation, linking temporal and spacial growth in the vicinity of the neutral stability line $\alpha_i \approx 0$, we propose the definition $c_g = \Re\left(\partial\omega/\partial\alpha\right)$ when considering stability in a region with significant exponents $\alpha_i \lesseqgtr 0$. This definition denotes a derivative of a real ω according to a complex α, which results in a generally complex expression and of which the real part $\Re$ is taken. The reason for this definition is, that the former definition, contrary to what one might spontaneously assume, will generally be a complex number. That is by the Cauchy-Riemann equations and the uniqueness of the underlying limit, defining the complex derivative,

$$\frac{\partial\omega}{\partial\alpha} = \lim_{h\to 0}\frac{\omega(\alpha+h)-\omega(\alpha)}{h} = \frac{\partial\omega}{\partial\alpha_r} = \frac{\partial\omega}{\partial(i\alpha_i)}, \quad (13)$$

for arbitrary $h \in \mathbb{C}$. However, the current study requires a real-valued quantity to assess the direction of energy transport.

The derivative $\partial\omega/\partial\alpha$ can be constructed from a first-order Taylor expansion of a complex dispersion relation $\mathcal{D} = 0$

$$\frac{\partial\omega}{\partial\alpha} = -\frac{\frac{\partial\mathcal{D}}{\partial\alpha}}{\frac{\partial\mathcal{D}}{\partial\omega}}. \quad (14)$$

The key instability condition implies that the group velocity must be in the direction of spatial growth. In 2D, the direction of wave propagation as well as growth/decay can only be in x-direction. Growth in the positive x-direction refers to a negative α_i and instability also implies that the group velocity c_g is in the same direction, i.e. in positive x-direction. For growth in the negative x-direction, both signs are reversed, i.e. the product of the two must always be negative for instability, i.e. we find

$$\Re\left(\frac{\partial\omega_{2D}}{\partial\alpha_{2D}}\right)\alpha_{2D,i} < 0. \quad (15)$$

For the 3D instability condition, the wave number vector as well as the group velocity vector consist of two components in the (x, z)-plane, which are transformed according to the extended Squire transformation (12)

$$\begin{pmatrix}\alpha_{3D}\\ \beta\end{pmatrix} = \begin{pmatrix}\frac{1}{\phi}\alpha_{2D}\\ \mp i\sqrt{\frac{1}{\phi^2}-1}\,\alpha_{2D}\end{pmatrix}, \quad (16a)$$

$$\begin{pmatrix}\frac{\partial\omega_{3D}}{\partial\alpha_{3D}}\\ \frac{\partial\omega_{3D}}{\partial\beta}\end{pmatrix} = \begin{pmatrix}\frac{\partial\omega_{2D}}{\partial\alpha_{2D}}\\ \mp\frac{1}{i\sqrt{1-\phi^2}}\frac{\partial\omega_{2D}}{\partial\alpha_{2D}}\end{pmatrix}. \quad (16b)$$

For a spatial 3D stability analysis, an oblique neutral stability line (NSL) is defined by

$$\alpha_{3D,i}x + \beta_i z = 0, \quad (17)$$

along which there is neither growth nor decay (see Figure 1), so that a corresponding neutral stability angle can be formulated as

$$\tan\theta_{NSL} = -\frac{\beta_i}{\alpha_{3D,i}} = \pm\sqrt{1-\phi^2}\,\frac{\alpha_{2D,r}}{\alpha_{2D,i}}, \quad (18)$$

i.e. the angle is obviously still inherently dependent on ϕ.

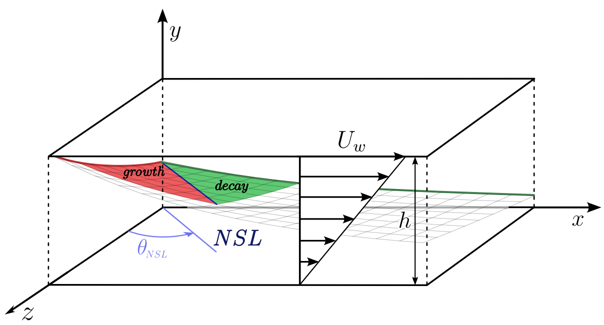

Figure 1. 3D oblique mode in plane Couette flow with areas of growth (red), decay (green) and the neutral stability line (NSL). Exemplary here: $\alpha_i > 0$, $\beta_i < 0$ and artificially set $\alpha_r = \beta_r = 0$ to increase visibility.

The above definitions show that for the 3D case, growth can only occur perpendicular to the NSL, and we want to introduce a correspondingly rotated coordinate system. Let the coordinate system rotate in the mathematically positive orientation around the y-axis with the neutral stability angle θ_{NSL}, so that the $\tilde{z}$-axis falls onto the neutral stability line (Figure 2).

$$\begin{pmatrix}\tilde{x}\\ \tilde{z}\end{pmatrix} = \begin{pmatrix}\cos\theta_{NSL} & -\sin\theta_{NSL}\\ \sin\theta_{NSL} & \cos\theta_{NSL}\end{pmatrix}\begin{pmatrix}x\\ z\end{pmatrix}. \quad (19)$$

The corresponding wave numbers in the new coordinate system take the form

$$\begin{pmatrix}\tilde{\alpha}_{3D}\\ \tilde{\beta}\end{pmatrix} = \begin{pmatrix}\cos\theta_{NSL} & -\sin\theta_{NSL}\\ \sin\theta_{NSL} & \cos\theta_{NSL}\end{pmatrix}\begin{pmatrix}\alpha_{3D}\\ \beta\end{pmatrix}. \quad (20)$$

Based on this, and per definition, spatial growth/decay only exists in $\tilde{x}$-direction, and a condition similar to the 2D

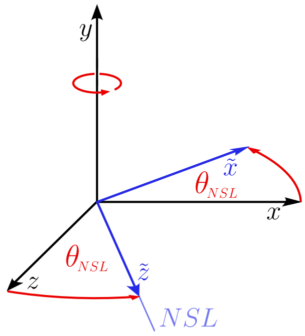

Figure 2. Rotation of the (x, z)-plane around the y-axis with the angle θ_{NSL} so that spatial growth/decay only exists in $\tilde{x}$-direction.

instability condition (15) can be formulated as

$$\Re\left(\frac{\partial \omega_{3D}}{\partial \tilde{\alpha}_{3D}}\right)\tilde{\alpha}_{3D,i} < 0. \tag{21}$$

Inserting the transformation of the wave numbers between the two coordinate systems, (20), into (21) gives the group-velocity based instability condition for the 3D case in the original coordinate system

$$\left[\Re\left(\frac{\partial \omega_{3D}}{\partial \alpha_{3D}}\right)\cos\theta_{NSL} - \Re\left(\frac{\partial \omega_{3D}}{\partial \beta}\right)\sin\theta_{NSL}\right] \cdot (\alpha_{3D,i}\cos\theta_{NSL} - \beta_i \sin\theta_{NSL}) < 0. \tag{22}$$

Furthermore, if the 3D quantities are replaced by the 2D quantities according to the relationships in (16a) and (16b) and the neutral stability angle θ_{NSL} given in (18) is used, the following 3D instability condition results

$$[(1-\phi^2)\alpha_{2D,r}^2 + \alpha_{2D,i}^2] \cdot \left[\Re\left(\frac{\partial \omega_{2D}}{\partial \alpha_{2D}}\right)\alpha_{2D,i} + \Im\left(\frac{\partial \omega_{2D}}{\partial \alpha_{2D}}\right)\alpha_{2D,r}\right] < 0, \tag{23}$$

where $\Im$ refers to the imaginary part of its argument,

As we here assumed $0 < \phi < 1$, the expression in the first bracket always remains positive, so that this 3D instability condition is reduced to

$$\Re\left(\frac{\partial \omega_{2D}}{\partial \alpha_{2D}}\right)\alpha_{2D,i} + \Im\left(\frac{\partial \omega_{2D}}{\partial \alpha_{2D}}\right)\alpha_{2D,r} < 0. \tag{24}$$

The first summand of (24) is equal to the 2D instability condition (15) and represents a condition for instability in the x-direction, while the second summand represents a condition for instability in the z-direction.

The significance of the combination of growth and decay in the two directions x and z is best seen in Figure 1, where one can see a decay in the positive x-direction, but growth in the positive z-direction. An instability is obviously only present, if the group velocity has a portion that points in the direction of overall growth, i.e. in the negative direction of $\tilde{x}$ when the new coordinate system is introduced according to Figure 2. This is the central statement of the group velocity condition (24) for 3D modes.

PLANE COUETTE FLOW: EIGENVALUE PROBLEM

As a first test case, we want to investigate whether 3D oblique modes exist for the plane Couette flow. This flow is special since no unstable temporally evolving 2D modes are known for it - presumably they do not exist. Here, we will investigate spatially evolving 2D modes by solving the corresponding eigenvalue problem and checking whether the 3D instability condition (24) is fulfilled for the respective mode.

The Couette geometry defines a shear flow between two parallel walls with a distance h, where the upper wall is moving tangentially in positive x-direction with the velocity U_w, while no pressure gradient is applied. Hence, we employ $L = h$ and $U_0 = U_w$ for non-dimensionalization. The no-slip boundary conditions on both walls then yield a linear velocity profile $U(y) = y$. This eliminates the second-order derivative term $\mathrm{d}^2U/\,\mathrm{d}y^2$ in the Orr-Sommerfeld equation (6).

With this, the Orr-Sommerfeld equation admits the exact analytical solution for the eigenfunction $\tilde{v}(y)$ (see e.g. Reid, 1979), i.e.

$$\tilde{v}(y) = C_1 e^{ky} - \frac{C_2}{2k}\left[e^{-ky} - e^{ky}\right] - \frac{C_3}{2k}\left[e^{-ky}Q_1 - e^{ky}Q_2\right] - \frac{C_4}{2k}\left[e^{-ky}Q_3 - e^{ky}Q_4\right], \tag{25a}$$

$$\text{with} \quad k^2 = \alpha^2 + \beta^2, \quad \text{and} \tag{25b}$$

$$Q_1(y) := \int_0^y e^{k\breve{y}} Ai(\sigma)\,\mathrm{d}\breve{y}, \quad Q_2(y) := \int_0^y e^{-k\breve{y}} Ai(\sigma)\,\mathrm{d}\breve{y}, \tag{25c}$$

$$Q_3(y) := \int_0^y e^{k\breve{y}} Bi(\sigma)\,\mathrm{d}\breve{y}, \quad Q_4(y) := \int_0^y e^{-k\breve{y}} Bi(\sigma)\,\mathrm{d}\breve{y}, \tag{25d}$$

$$\text{and} \quad \sigma(\breve{y}) := \frac{(-i\alpha Re)^{\frac{1}{3}}\left(-\alpha\breve{y}Re + \omega Re + ik^2\right)}{\alpha Re}, \tag{25e}$$

where Ai, Bi denote the Airy functions. With the non-permeable wall and the no-slip boundary conditions

$$\tilde{v}(y=0) = 0, \quad \tilde{v}(y=1) = 0, \tag{26a}$$

$$\frac{\mathrm{d}}{\mathrm{d}y}\tilde{v}(y=0) = 0, \quad \frac{\mathrm{d}}{\mathrm{d}y}\tilde{v}(y=1) = 0, \tag{26b}$$

an eigenvalue problem can be formulated as

$$\underbrace{\begin{pmatrix} 1 & 0 & 0 & 0 \\ e^k & \frac{-e^{-k}+e^k}{2k} & \frac{-e^{-k}\tilde{Q}_1+e^k\tilde{Q}_2}{2k} & \frac{-e^{-k}\tilde{Q}_3+e^k\tilde{Q}_4}{2k} \\ k & 1 & 0 & 0 \\ ke^k & \frac{e^{-k}+e^k}{2} & \frac{e^{-k}\tilde{Q}_1+e^k\tilde{Q}_2}{2} & \frac{e^{-k}\tilde{Q}_3+e^k\tilde{Q}_4}{2} \end{pmatrix}}_{\boldsymbol{D}} \cdot (C_1, C_2, C_3, C_4)^{\mathsf{T}} = (0,0,0,0)^{\mathsf{T}} \tag{27}$$

with $\tilde{Q}_i = Q_i(y = 1)$. This equation yields a non-trivial solution only if the determinant of $\boldsymbol{D}$ vanishes, i.e. we obtain the dispersion relation $\mathcal{D}$ for the plane Couette flow

$$\mathcal{D} = \det \boldsymbol{D} = 0, \tag{28}$$

which can be thus be expressed as

$$\mathcal{D} = \int_0^1 e^{k\breve{y}} Ai(\sigma)\,\mathrm{d}\breve{y} \int_0^1 e^{-k\breve{y}} Bi(\sigma)\,\mathrm{d}\breve{y} - \int_0^1 e^{k\breve{y}} Bi(\sigma)\,\mathrm{d}\breve{y} \int_0^1 e^{-k\breve{y}} Ai(\sigma)\,\mathrm{d}\breve{y} = 0. \quad (29)$$

This eigenvalue problem is computed in 2D and then transformed to 3D according to the extended Squire transformation (12), since it is easier to compute in 2D.

A highly accurate calculation scheme for computing the eigenvalues is set up and consists of a two-stage algorithm. In the first step, the eigenvalue spectrum for a given Re_{2D} and ω_{2D} is numerically approximated by a Chebyshev collocation method applied to (7) and (26), formulated by Sun (2020), who modified the spatial stability collocation code of Schmid & Henningson (2001) using Ye *et al.* (2016).

In order to obtain reliable and particularly precise eigenvalues in a second step, a reiteration scheme for the eigenvalues has been developed by Laux (2023) using Muller's method for complex root-finding (Muller, 1956), which at the same time eliminates spurious modes that appear due to the collocation code. The code has been extended to arbitrary precision arithmetic, i.e. an unrestricted number of decimal places, by a combination of the programming languages, *Julia* (Bezanson *et al.*, 2017), and *Python* (van Rossum, 1995). The eigenvalues α_{2D} of the collocation method are inserted into the analytical dispersion relation (29) $\mathcal{D}_{2D} = 0$, where only the integrals in (29) have to be evaluated numerically, using a high arbitrary precision arithmetic of 128 decimal places by default. The evaluation of these integrals is accepted, if the estimated errors of these evaluations are smaller than the last decimal place with which the calculations were performed. Otherwise, the number of decimal places is increased, and the evaluation of the integrals is performed again. Muller's method iterates the eigenvalues until the residuum of the dispersion relation is considered negligibly small. Here, this is assumed when the residuum is smaller than the last default decimal place, i.e. smaller than 10^{-128}.

In Figure 3, a large section of the reiterated eigenvalue spectrum for the parameter combination $Re_{2D} = 350$, $\omega_{2D} = 0.1$ is shown. Regions of eigenvalues have been given intuitive names, i.e. there are two *parabolic branches* in the positive imaginary half-plane, a *linear branch* in the negative imaginary half-plane, slightly inclined to the real axis, and two *hyperbolic branches* in the negative imaginary half-plane.

In Figure 4, a section of the reiterated eigenvalue spectrum for $Re_{2D} = 2800$ and varying ω_{2D} near the origin is shown. An angular wave frequency of $\omega_{2D} = 0$ would correspond to an eigenvalue spectrum axisymmetric to the imaginary axis, but this describes a non-periodic phenomenon. A positive ω_{2D} breaks this symmetry by shifting the eigenvalues to the right and a bit up with increasing ω_{2D}.

In Figure 5, a section of the reiterated eigenvalue spectrum for varying Re_{2D} and $\omega_{2D} = 0.25$ near the origin is shown. With increasing Re_{2D}, the eigenvalues are shifted to the inside of the two parabolic branches.

In Figure 6, a section of the reiterated eigenvalue spectrum near the origin for the parameter combination $Re_{2D} = 2800$ and $\omega_{2D} = 0.1$ is shown. Additionally, the eigenvalues fulfilling the 2D and 3D instability condition (15) and (24) are marked as unstable for 2D and 3D. The linear branch of eigenvalues is always unstable with both the 2D and 3D instability condition. One eigenvalue in the negative real half-plane is also unstable in both 2D and 3D. However, there is one eigenvalue in the positive imaginary half-plane that is stable in 2D but becomes unstable with the 3D instability condition.

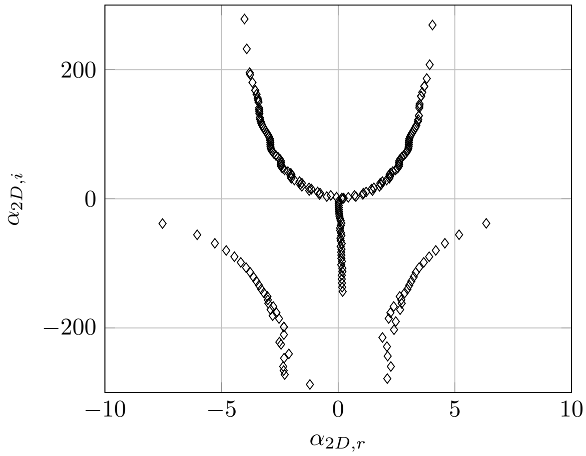

Figure 3. Reiterated eigenvalue spectrum for $Re_{2D} = 350$, $\omega_{2D} = 0.1$.

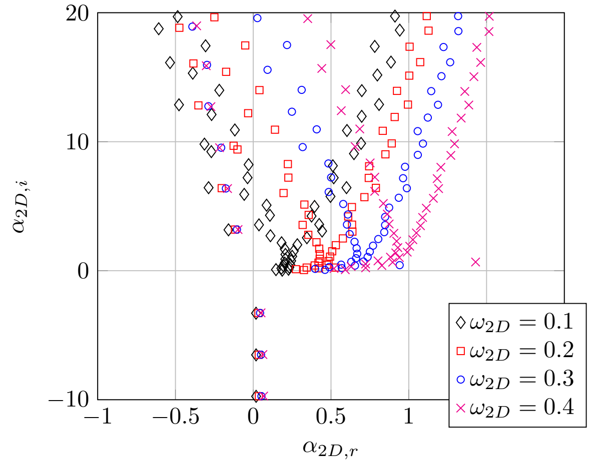

Figure 4. Reiterated eigenvalue spectrum for $Re_{2D} = 2800$ and varying ω_{2D}.

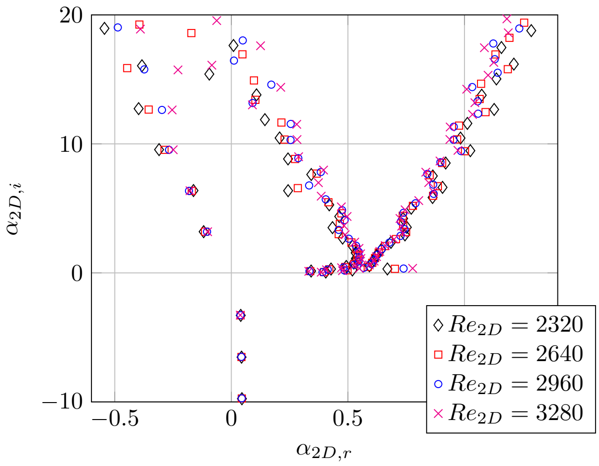

Figure 5. Reiterated eigenvalue spectrum for varying Re_{2D} and $\omega_{2D} = 0.25$.

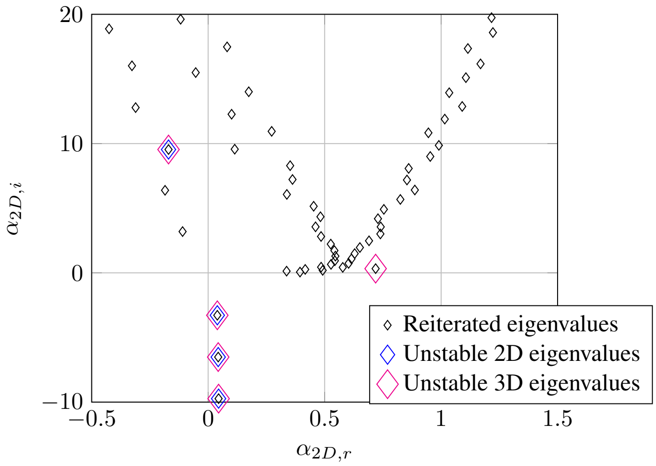

Figure 6. Reiterated eigenvalue spectrum for $Re_{2D} = 2800$, $\omega_{2D} = 0.25$, and unstable 2D and 3D eigenvalues based on (15) and (24).

CONCLUSIONS AND OUTLOOK

By extending the Squire transformation to the spatial stability framework, it was shown that spatial instabilities in 3D can appear at lower Reynolds numbers than in 2D and must therefore be considered in the stability analysis. The extended Squire transformation furthermore allows performing the 3D stability analysis using the corresponding 2D quantities. The group velocity as an important property of spatial stability has been included in the considerations for an instability condition. An instability condition for 3D has been formulated using the corresponding 2D quantities.

By investigating the spatial linear stability eigenvalue problem of plane Couette flow, it was shown that there exist spatially growing 3D modes in the lower as well as in the upper half-plane of the complex α_{2D}-plane. Some modes appear to be unstable both in 2D and 3D, while other modes are stable for 2D, but unstable for 3D. This underlines the findings of the extended Squire transformation that there might exist unstable 3D modes at lower critical Reynolds numbers than for 2D modes, i.e. modes at a given Reynolds number unstable in 3D but stable in 2D. A mode stable in 3D but unstable in 2D has not been found yet.

The next step is to thoroughly investigate the parameter space ω_{2D}, Re_{2D} and the scaling parameter ϕ, to find eigenvalues corresponding to the experimentally observed oblique structures in the transition from laminar to turbulent state, and to perform DNS on these eigenvalues.

The authors would like to acknowledge Judith Schulz for creating the beautiful Figures 1 and 2.

REFERENCES

Bezanson, J., Edelman, A., Karpinski, S. & Shah, V. B. 2017 Julia: A Fresh Approach to Numerical Computing. *SIAM Review* **59** (1), 65–98.

Criminale, W. O., Jackson, T. L. & Joslin, R. D. 2010 *Theory and Computation of Hydrodynamic Stability*. Cambridge University Press.

Daviaud, F., Hegseth, J. & Bergé, P. 1992 Subcritical transition to turbulence in plane Couette flow. *Physical review letters* **69** (17), 2511–2514.

Laux, J. 2023 Analysis of oblique 3D modes in plane shear flows. Master's thesis, Technische Universität Darmstadt, Darmstadt.

Muller, D. E. 1956 A method for solving algebraic equations using an automatic computer. *Mathematics of Computation* **10** (56), 208–215.

Prigent, A., Grégoire, G., Chaté, H. & Dauchot, O. 2003 Long-wavelength modulation of turbulent shear flows. *Physica D: Nonlinear Phenomena* **174** (1-4), 100–113.

Reid, W. H. 1979 An Exact Solution of the Orr–Sommerfeld Equation for Plane Couette Flow. *Studies in Applied Mathematics* **61** (1), 83–91.

Romanov, V. A. 1973 Stability of plane-parallel Couette flow. *Functional Analysis and Its Applications* **7** (2), 137–146.

Schmid, P. J. & Henningson, D. S. 2001 *Stability and Transition in Shear Flows*, *Applied Mathematical Sciences*, vol. 142. New York and Berlin and Heidelberg: Springer.

Squire, H. B. 1933 On the stability for three-dimensional disturbances of viscous fluid flow between parallel walls. *Proceedings of the Royal Society of London. Series A, Containing Papers of a Mathematical and Physical Character* **142** (847), 621–628.

Sun, W. 2020 Dreidimensionale Stabilitätsanalyse einer ebenen Couette-Strömung mit Wandtranspiration. Master's thesis, Technische Universität Darmstadt, Darmstadt.

Tillmark, N. & Alfredsson, P. H. 1992 Experiments on transition in plane Couette flow. *Journal of Fluid Mechanics* **235** (-1), 89.

Tillmark, N. & Alfredsson, P. H. 1993 Turbulence in plane Couette flow. *Applied Scientific Research* **51** (1-2), 237–241.

Tuckerman, L. S. & Barkley, D. 2011 Patterns and dynamics in transitional plane Couette flow. *Physics of Fluids* **23** (4), 014501.

Tuckerman, L. S., Chantry, M. & Barkley, D. 2020 Patterns in Wall-Bounded Shear Flows. *Annual Review of Fluid Mechanics* **52** (1), 343–367.

van Rossum, G. 1995 *Python Reference Manual*. Centrum voor Wiskunde en Informatica. Department of Computer Science: Amsterdam.

Ye, H.-Y., Yang, L.-J. & Fu, Q.-F. 2016 Spatial instability of viscous double-layer liquid sheets. *Physics of Fluids* **10** (28).